STUDIES OF FERRITE MATERIALS FOR THE AGS BOOSTER SYNCHROTRON

M.A. Goldman, P. Cameron, R.T. Sanders and J. Tuozzolo
BROOKHAVEN NATIONAL LABORATORY
Upton, New York 11973

Abstract

The BNL Booster Synchrotron will inject heavy ion and proton beams of increased intensity into the Alternating Gradient Synchrotron. Its accelerating cavities are sweep-tuned by varying the permeability of ferrite core rings within the cavities. Core material selection criteria and evaluation are discussed. Measurements of permeability, loss and permittivity are presented.

Introduction

The heavy ion cavities will operate at (I) 0.175-0.68 MHz and (II) 0.67-2.5 MHz; the proton cavities will operate at (III) 2.4-4.2 MHz, and are described in [1]. To attain voltages originally scheduled in [1] a B x f product (proportional to voltage per unit cross-section area of ferrite) of 115 Gauss x MHz is desired for ferrites in frequency bands I, II and 375 Gauss x MHz for band III. During acceleration, the core inductance should vary as $1/f^2$ to resonate with cavity gap capacitors. This is done by programming a DC bias current to control the polarizing magnetic field, $\bar{H}_p$, in the cores.

For band I a high permeability ferrite ($\mu \approx 1,400$ at 0.18 MHz) is needed, both to attain a high B x f product and to avoid an excessive volume of high voltage capacitors at the gap.

In contrast, a low-μ ferrite ($\mu \approx 110$ at 2.5 MHz) is needed for III to achieve required gap voltage without excessive loss while allowing the presence of sufficient gap capacitance to avoid excitation of Robinson's instability [2] by the intense proton beam.

A study of candidate materials led to a choice of TDK type SY7, a 1:2 Ni-Zn ferrite for I, II and Philips type 4M2, a 6:4 Ni-Zn spinel, for III. High-μ Mn-Zn ferrites tested for possible use in I had excessive loss. In the sections below we outline measurement methods for ferrite evaluation and present some of our measured results.

Ferrite Evaluation

Candidate materials were screened by measuring mean permeability, $\bar{\mu}_\Delta$ and power loss/volume, P_D/V, of small sample rings, in the test cavity of Fig. 1, using the circuit of Fig. 2.

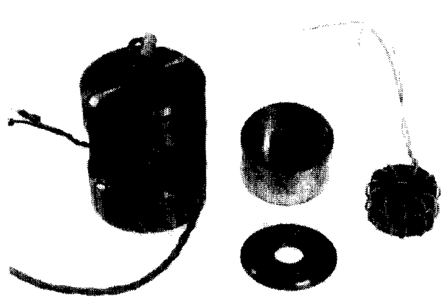

Fig. 1 Small Sample Evaluation Test Cavity

* Work performed under the auspices of the U.S. Dept. of Energy.

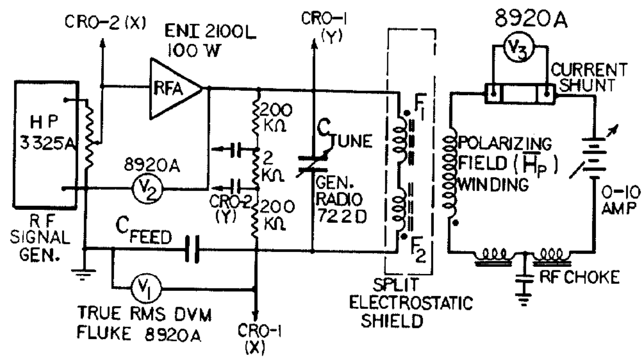

Fig. 2 Measurement Circuit for the Small Sample Cavity

Two rings are series connected by a figure-8 winding which is electrostatically shielded and magnetically decoupled from the H_P winding. The feed capacitor is several times larger than the tuning capacitor. The cavity is resonated by varying the precision tuning capacitor to give minimum voltage across the feed capacitor; the RF voltages across these capacitors will then be close to quadrature. The mean RF permeability $\bar{\mu}_\Delta$, peak RF area-averaged B-field, B_{RF}peak, and loss are obtained from the resonance voltages across the RMS voltmeters V_1 and V_2. Before RF measurements are made, the rings are initially polarized by cycling $\bar{H}_P$ between remanence and saturation. A thermally controlled oil bath allows constant temperature measurements to be made. Fig's. 3, 4 show typical behavior of permeability and loss for small SY7 sample rings.

Fig. 3 Typical Variation of Permeability at Constant Frequency and Polarizing Field.

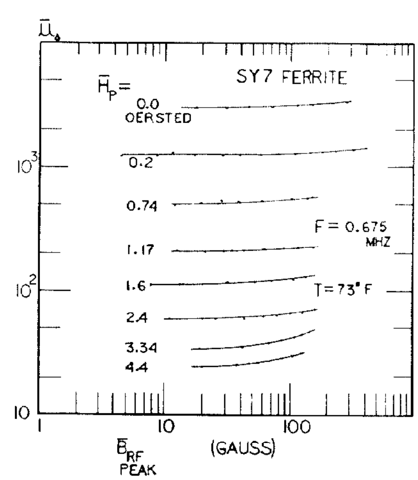

CH2669-0/89/0000-0165$01.00©1989 IEEE

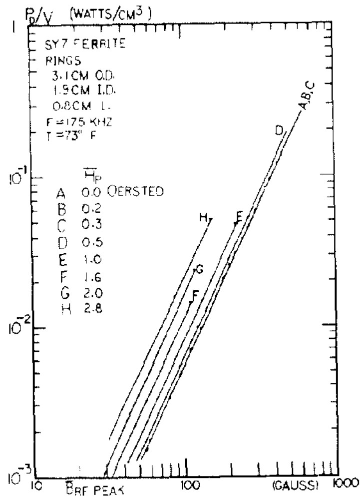

Fig. 4 Typical Loss Dependence on RF Flux Density and Polarizing Magnetic Field Intensity

Measured permeability scales well to larger ring size but loss is larger for full size rings (50 cm OD) at comparable B_{RF}. Part of the loss increase is due to eddy current contribution, which is disproportionately greater in large rings. The 4M2 material has negligible RF conductivity and eddy loss. The SY7 is semiconducting and shows strong temperature and frequency dependence of resistivity. In order to estimate eddy loss the material's RF resistivity and complex permitivity were measured (Figs. 5-7). The RF resistivity of SY7 is at least an order of magnitude greater than that of any Mn-Zn ferrite tested.

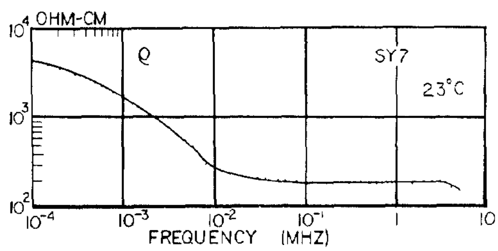

Fig. 5 RF Resistivity of SY7 Ferrite

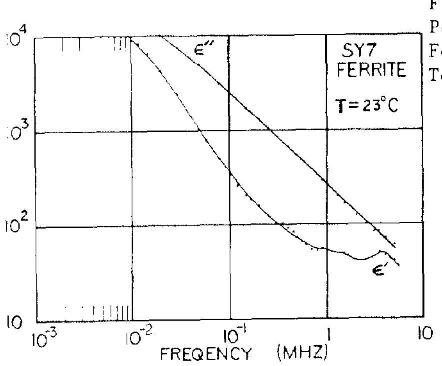

Fig. 6 Complex Permittivity of SY7 Ferrite at Room Temperature

Full sized rings are studied in a 2-ring cavity configured so that the rings lie in separate annular cavities, electrically in parallel; bias current counter-couples so as to cancel induction between the bias and RF current paths (Fig. 8). The resonant RF current is sampled by a Pearson model 110 current transformer via a breakout box in the coaxial RF feed line, and RF voltage is sampled by a capacitive voltage divider, each terminated in an RMS digital voltmeter to allow power measurement. To date, measurements were made at fixed tuning capacitance and frequency. Swept loss measurements are being made; it is expected that these will give higher loss because of domain wall motion processes associated with variation of H_p.

Fig. 7 Temperature Dependence of SY7 RF Resistivity

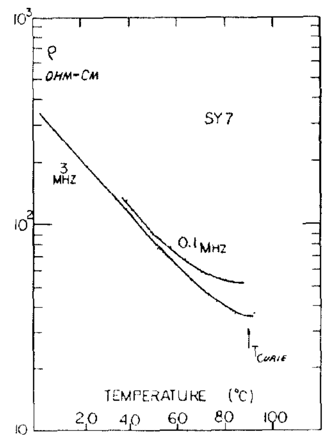

Measurement Results

In both large and small rings of SY7 the loss varied as $B_{rf}^{2.07\pm.05}$, measured at constant bias field intensity, for a wide range of B_{rf} and H_p; loss increases monotonically and rapidly with H_p when measured at constant B_{rf} and frequency. This behavior holds even up to the onset of magnetic instabilities (when the material's domain structure changes under the influence of large RF excitation). In the 4M2, loss varies also as $B_{rf}^{2.07}$ at low and moderate B_{rf}, but at large RF flux density shows a saturation behavior; loss increases rapidly as B_{rf} increases towards a saturation value which depends upon H_p.(Fig.9)

Fig. 9 Large Ring Static Loss Versus RF Induction Field, For Band III Bias Schedule

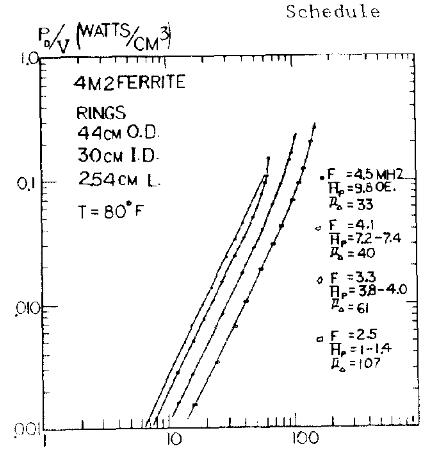

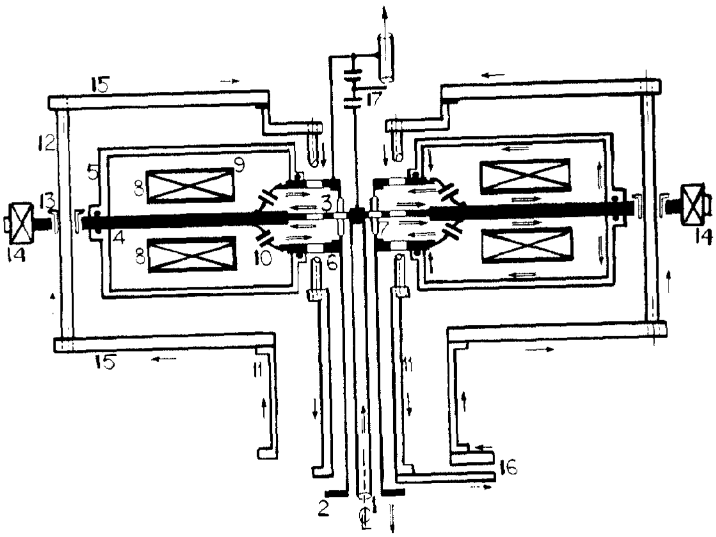

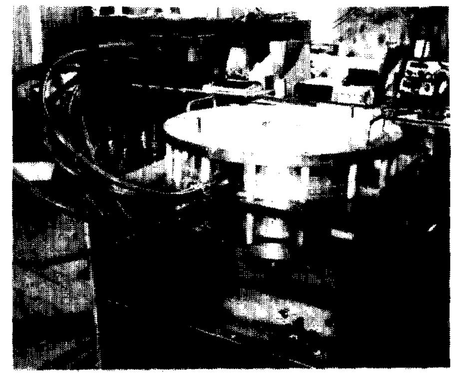

Fig. 8 Two-Ring Test Cavity for Full Sized Ferrite

1, 2. Coaxial RF Feed Electrode
3. Cruciform RF Feed Through Slotted Coaxial Electrode
4. Copper Midplane Plate
5. Resonator Cavity Pan
6. RF Feed Disc from Outer Coax Feed to Pan
7. Slotted Extension of Coaxial Outer Electrode
8. Ferrite Rings
9. Water Cooling Plates
10. Ceramic Tuning Capacitors
11. Bias Current Feed Tubes
12. Bias Current Feed Rod Array
13. Insulating Bushing
14. Bearing Pillow Blocks to Allow Cavity Inversion for Ferrite Installation
15. Cover Plates Carrying Bias Current
16. Lug Plates for Bias Current Feed
17. 50:1 Capacitive Voltage Divider

Fig. 10 shows measured loss for a band (II) drive schedule. The SY7 rings achieved 115 Gauss x MHz operation in band II without onset of instability, but only achieved half this Bf product in band I when operating over essentially the same bias field range (.16-1.8 and 0.1-1.7 Oe respectively). Onset of instability rather than excessive loss may limit the band I operating voltage; in this case the cavity could operate at lower voltage for longer acceleration time. The 4M2 material operated steady at 375 Gauss x MHz over the lower half of band III but came close to thermal loss limits (0.3 watt/cm^3 average) and instability over the upper half of the band; the accelerating cavity design has been modified to use ramped decreasing accelerating voltage over this half band, with modified proton beam synchronous phase angle.

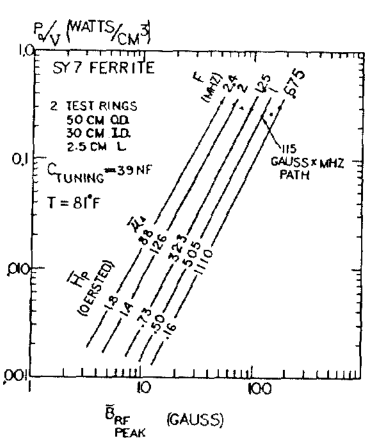

Fig. 10 Large Ring Static Loss for Proposed Booster Band II Drive Schedule

At moderate B_{RF} the ferrites have behaved as lossy inductors, but at large B_{RF} they show complex behavior, whose nature depends upon the particular excitation conditions. Magnetic aftereffect, 2-frequency quasiperiodic oscillation in cavity current with beat period of several milliseconds and, at large drive, fully developed chaotic behavior have all been observed. These phenomena are being investigated in further studies.

Acknowledgements

The authors wish to acknowledge extensive discussions with Martin Plotkin and Klaus Kaspar which contributed to the measurements. They thank John Bunicci, Nick Laloudakis and Alex Zaltsman for implementing the power amplifier electronics, Mikhael Pritsker and Steve Gutstein for contributions to the measurements and planning and thank A. McNerney and W. T. Weng for management support and encouragement.

References

[1] R. Sanders, et al., Proc. European Particle Accelerator Conf. Rome, Italy June 7-11, 1988.
[2] K. W. Robinson, Cambridge Electron Accelerator Report CEAL-1010, 1964.